

Anterior condylar arteriovenous fistula mainly fed by peripheral branches of the bilateral internal maxillary arteries: illustrative case

Genki Kimura, MD, Hiroyuki Ikeda, MD, PhD, Ryosuke Nishi, MD, Hidenobu Hata, MD, Minami Uezato, MD, Masanori Kinoshita, MD, Yoshitaka Kurosaki, MD, PhD, and Masaki Chin, MD

Department of Neurosurgery, Kurashiki Central Hospital, Kurashiki, Japan

BACKGROUND The main feeding artery of an anterior condylar arteriovenous fistula (AC-AVF) is the ascending pharyngeal artery and rarely the internal maxillary artery.

OBSERVATIONS A 58-year-old male with a history of sinusitis since adolescence presented with a 5-year history of bilateral pulsatile tinnitus and a 2-month history of right ocular symptoms. Angiography showed that the peripheral branches of the bilateral internal maxillary arteries were the main feeding arteries of the AC-AVF and that they gathered in the clivus with a relatively large shunted pouch in the left jugular tubercle. Shunt flow drained to the right external jugular vein via the right superior ophthalmic vein. A sheath was placed in the right external jugular vein, and a small distal access catheter was guided to the right superior ophthalmic vein to allow the microcatheter to reach the shunted pouch. Selective angiography of the contralateral sphenopalatine artery allowed us to confirm the gathering site of the feeding arteries and the shunted pouch and archive the complete occlusion.

LESSONS Selective angiography of the contralateral sphenopalatine artery may be useful to confirm the gathering site of the peripheral branches of the bilateral internal maxillary arteries in an AC-AVF.

<https://thejns.org/doi/abs/10.3171/CASE23452>

KEYWORDS anterior condylar; arteriovenous fistula; embolization; maxillary artery; sphenopalatine artery

Anterior condylar-arteriovenous fistula (AC-AVF) is a relatively rare AVF that forms around the hypoglossal canal. In an AC-AVF, the main feeding artery is often the ascending pharyngeal artery, which runs near the hypoglossal canal, and is rarely the internal maxillary artery.^{1–4} We report the case of an AVF for which the main feeding artery was the bilateral internal maxillary arteries.

Illustrative Case

History and Examination

A 58-year-old male had hypertension, hyperuricemia, and a history of chronic sinusitis since adolescence but no history of head and neck trauma or surgery. He presented with a 5-year history of bilateral pulsatile tinnitus and a 2-month history of conjunctival hyperemia, proptosis, and abducens nerve disease in the right eye. Magnetic resonance angiography showed high signal intensity in the left jugular tubercle and intraosseous part of the clivus and faint

high signal intensity in the left anterior condylar vein and right cavernous sinus, suggesting a left AC-AVF (Fig. 1A and B). Computed tomography showed the loss of cancellous bone in the left jugular tubercle and left maxillary sinusitis (Fig. 1C). A fusion image of computed tomography angiography and venography showed that the outflow from the shunted pouch of the left AC-AVF drained into the right superior ophthalmic vein via the right cavernous sinus. (Fig. 1D).

The left external carotid angiography showed that the sphenopalatine artery, the artery of the foramen rotundum, and the artery of the pterygoid canal, which are peripheral branches of the internal maxillary artery, mainly flowed into the left AC-AVF. The cavernous sinus branch of the middle meningeal artery, the accessory meningeal artery, and the ascending pharyngeal artery also flowed into the shunted pouch (Fig. 2A–C). Outflow was divided into two directions of the anterior condylar vein and the basilar plexus from the

ABBREVIATIONS AC = anterior condylar; AVF = arteriovenous fistula.

INCLUDE WHEN CITING Published October 9, 2023; DOI: 10.3171/CASE23452.

SUBMITTED August 15, 2023. **ACCEPTED** September 6, 2023.

© 2023 The authors, CC BY-NC-ND 4.0 (<http://creativecommons.org/licenses/by-nc-nd/4.0/>)

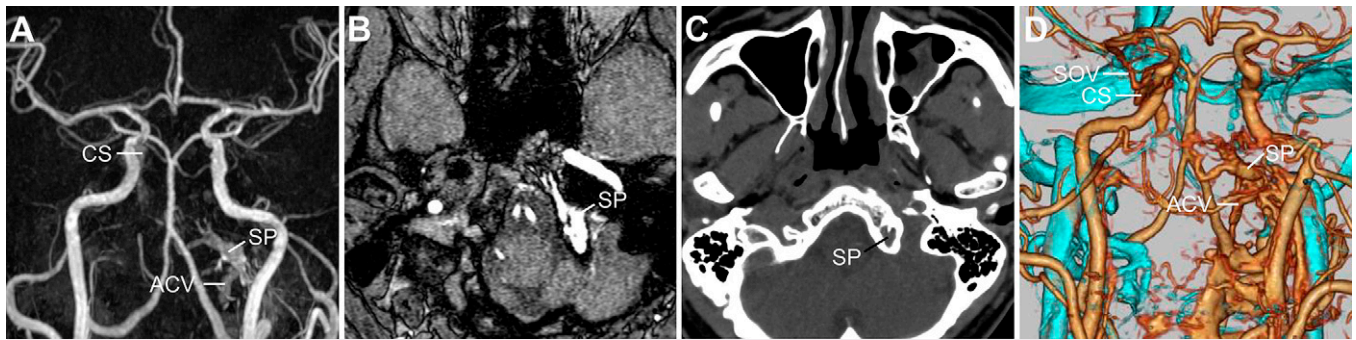


FIG. 1. Preoperative magnetic resonance angiography (MRA) and computed tomography (CT) images. **A:** MRA showing high signal intensity in the shunted pouch (SP) of the left AC-AVF and faint high signal intensity in the left anterior condylar vein (ACV) and right cavernous sinus (CS) as the outflow tracts. **B:** Time-of-flight (TOF) MRA image showing the SP of the left AC-AVF in the left jugular tubercle. **C:** CT showing the loss of cancellous bone in the SP of the left jugular tubercle and left maxillary sinusitis. **D:** A CT angiography (orange) and venography (blue) fusion image showing the SP of the left AC-AVF and outflow via the right CS into the right superior ophthalmic vein (SOV).

shunted pouch. Furthermore, blood flow from the basilar plexus was divided into two pathways, one draining from the right inferior petrosal sinus to the right internal jugular vein and the other draining through the right cavernous sinus, right superior ophthalmic vein, and right facial vein to the right external jugular vein. Blood flow from the left anterior condylar vein flowed to the left lateral condylar vein and the left posterior condylar vein, and downstream the blood flow was divided into the vertebral venous plexus and the deep cervical vein via the suboccipital cavernous sinus. On the other hand, blood flow from the left anterior condylar confluence formed a return pathway that flowed directly to the left internal jugular vein, in addition to a return pathway via the prevertebral vein to the right internal jugular vein. Selective angiography of the left sphenopalatine artery showed numerous feeding arteries that gathered and flowed into the shunted pouch from the medial side (Fig. 2D). Right external carotid angiography showed that the sphenopalatine artery, artery of the foramen rotundum, artery of the pterygoid canal, accessory meningeal artery, and ascending pharyngeal artery gathered in the clivus from the sphenoid bone to the occipital bone and flowed from the medial side into the shunted pouch within the left jugular tubercle (Fig. 2E and F). Selective angiography of the right sphenopalatine artery showed that the feeding arteries gathered and flowed into the shunted pouch from the medial side (Fig. 2G). Selective angiography of the left ascending pharyngeal artery showed diffuse inflow into the shunted pouch from the anterior caudal side (Fig. 2H and I). No cortical venous reflux was observed, and a diagnosis of AC-AVF (Borden type I, Cognard type IIa) was made.

Endovascular Surgery

Transvenous embolization was performed with the patient under general anesthesia. A 6-Fr guide catheter was placed in the bilateral external carotid arteries for intraoperative angiography during transvenous embolization, and a microcatheter was placed in the right sphenopalatine artery and left ascending pharyngeal artery, respectively, for selective angiography. First, we tried to reach the shunted pouch from the right femoral vein via the right internal jugular vein, right inferior petrosal sinus, and basilar plexus, but the microcatheter showed bending behavior in the right cavernous sinus and we could not reach the shunted pouch. Next, we tried to approach the right external jugular vein from the right subclavian vein, but the bifurcation angle of the right external jugular vein from the

right subclavian vein was very steep, making it difficult to select the right external jugular vein. The pathways from the vertebral venous plexus and the left deep cervical vein to the shunted pouch via the left anterior condylar vein were also very tortuous, and it was difficult to approach the shunted pouch via these pathways. Therefore, direct puncture of the right external jugular vein was chosen, an ultrasound-guided direct puncture was performed, and a 6-Fr short sheath was placed. We then introduced a small-diameter distal access catheter (3.2/3.4-Fr Guidepost, Tokai Medical Products) and a microcatheter (Headway Duo, Terumo) guided by a microguidewire (Chikai 14, Asahi Intecc). A distal access catheter was placed via the right facial vein into the right superior ophthalmic vein, and then a microcatheter was advanced via the right cavernous sinus, right inferior petrosal sinus, and basilar plexus into the shunted pouch (Fig. 3A). A microcatheter was advanced to the lateral posterior portion of the shunted pouch, where the left ascending pharyngeal artery gathered, and coil embolization was performed. We then reversed the microcatheter within the shunted pouch and guided it to the most proximal side of the gathering site of the peripheral branches of the bilateral internal maxillary arteries (Fig. 3B). Selective angiography of the right sphenopalatine artery showed that the microcatheter tip was located at the most proximal side of the gathering site of the feeding arteries (Fig. 3C), which was densely embolized (Fig. 3D). Selective angiography of the right sphenopalatine artery after embolization confirmed the disappearance of shunt blood flow (Fig. 3E). Selective angiography of the left ascending pharyngeal artery showed residual shunt blood flow to the shunted pouch, so we continued to embolize the shunted pouch and basilar plexus, which was considered the outflow from the shunted pouch (Fig. 3F). Right external carotid angiography, selective angiography of the left sphenopalatine artery, and left external carotid angiography each confirmed complete occlusion of the shunt (Fig. 3G–I), and the operation was completed.

Postoperative Course

There were no new findings of neurological symptoms in the postoperative period, and the right-eye conjunctival hyperemia and bilateral tinnitus disappeared immediately after the operation. The swelling and protrusion of the right eyelid disappeared the day after operation, and the abducens nerve disease in the right eye improved over time. Magnetic resonance angiography and time-of-flight imaging performed on the second postoperative day confirmed the disappearance of the

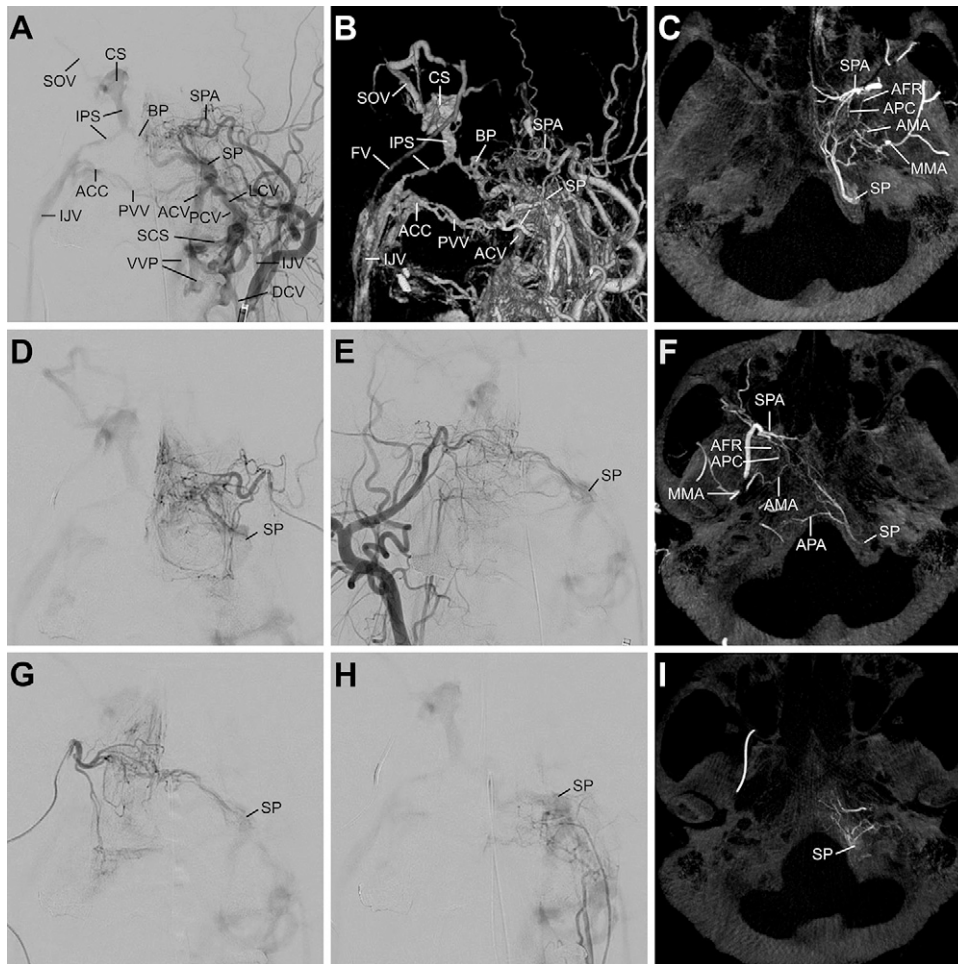


FIG. 2. Preoperative angiography images. Frontal view of angiography (A) and three-dimensional (3D) rotational angiography of the left external carotid artery (B) showing the left AC-AVF with the peripheral branches of the left internal maxillary artery as the main feeding arteries. Axial view of cone-beam CT reconstructed from 3D rotational angiography (C) of the left external carotid artery showing the sphenopalatine artery (SPA), artery of pterygoid canal (APC), artery of foramen rotundum (AFR), accessory meningeal artery (AMA), and CS branch of the MMA gathering in the sphenoid bone and the clivus of the occipital bone and flowing into the SP in the left jugular tubercle. Frontal view of selective angiography (D) of the left SPA showing the feeding arteries gathering and flowing into the SP. Frontal view of angiography (E) of the right external carotid artery showing the left AC-AVF with the peripheral branches of the right internal maxillary artery being the main feeding arteries. Axial view of cone-beam CT reconstructed from 3D rotational angiography (F) of the right external carotid artery showing the SPA, APC, AFR, AMA, and ascending pharyngeal artery (APA) gathering in the sphenoid bone and the clivus of the occipital bone and flowing into the SP in the left jugular tubercle. Frontal view of selective angiography (G) of the right SPA showing the feeding arteries gathering and flowing into the SP. Frontal view of selective angiography of the left APA (H) and axial view of cone-beam CT reconstructed from 3D rotational angiography of the left APA (I) showing the feeding arteries diffusely flowing into the SP from the anterior caudal side. ACC = anterior condylar confluence; BP = basilar plexus; DCV = deep cervical vein; FV = facial vein; IJV = internal jugular vein; IPS = inferior petrosal sinus; LCV = lateral condylar vein; MMA = middle meningeal artery; PCV = posterior condylar vein; PVV = prevertebral vein; SCS = suboccipital cavernous sinus; SOV = superior ophthalmic vein; SP = shunted pouch; VVP = vertebral venous plexus.

high signal intensity in the shunted pouch in the left jugular tubercle observed preoperatively (Fig. 4A and B). Computed tomography showed coil masses filling the gathering site of the peripheral branches of the bilateral internal maxillary arteries in the caudal side of the sphenoid bone, the shunted pouch in the jugular tubercle and the clivus

bone (Fig. 4C and D). Thereafter, the abducens nerve disease in the right eye disappeared completely, and the patient was discharged home on the fourth postoperative day. Magnetic resonance imaging was performed on an outpatient basis, and postoperative angiography performed at 6 months confirmed complete occlusion of the AVF.

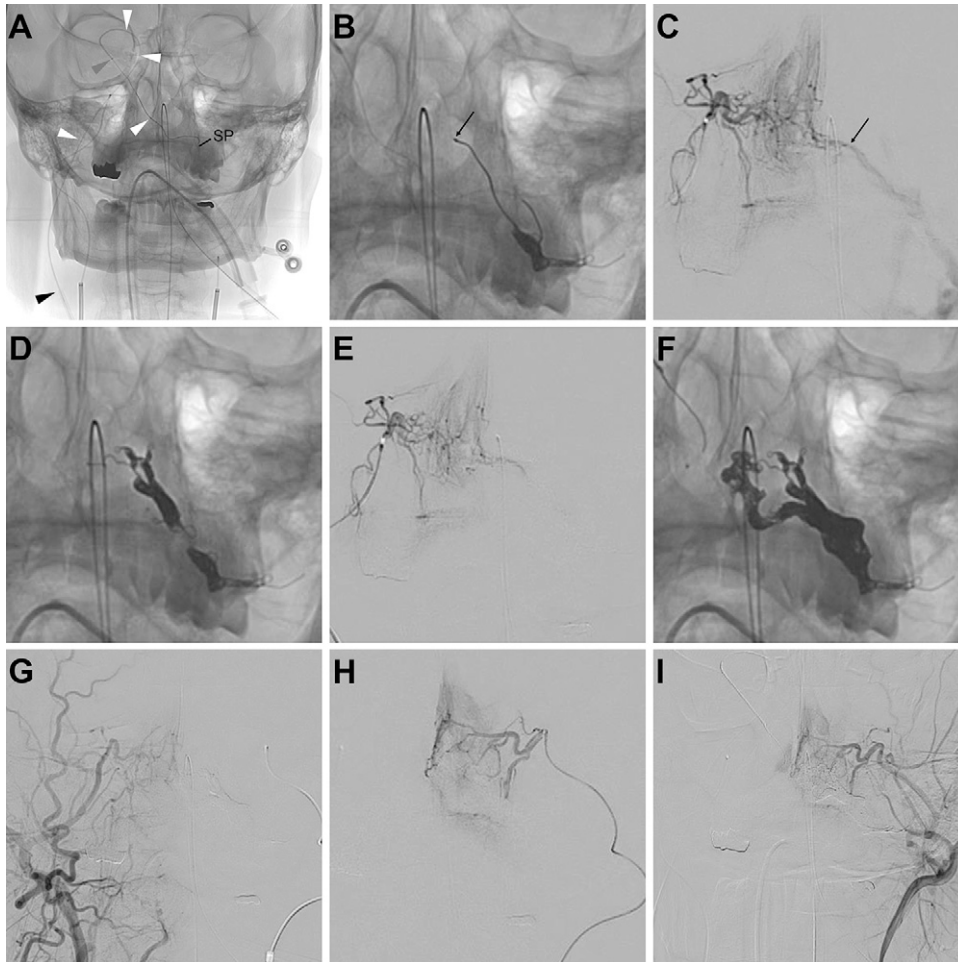


FIG. 3. Intraoperative imaging findings. A sheath was inserted directly into the right external jugular vein (*black arrowhead* is the tip of the sheath, **A**) and a small-diameter distal access catheter was placed in the right SOV via the right facial vein (*gray arrowhead*). A microcatheter was guided to the SP via the right cavernous sinus and basilar plexus using the distal access catheter. *White arrowheads* indicate access routes. After embolization of the lateral posterior portion of the SP, the microcatheter was reversed within the SP and guided to the most proximal side (*arrow*, **B**) of the gathering site of the peripheral branches of the bilateral internal maxillary arteries. Selective angiography of the right SPA (**C**) confirmed the presence of the microcatheter tip (*arrow*) for embolization at the most proximal side of the gathering site of the feeding arteries. The gathering site of the peripheral branches of the bilateral internal maxillary arteries was densely embolized with coils (**D**). Frontal view of selective angiography of the right SPA (**E**) after coil embolization of the gathering site of the peripheral branches of the bilateral internal maxillary arteries showing the disappearance of shunt blood flow. The SP and its outflow tract, the basilar plexus, were embolized with coils (**F**). Right external carotid angiography (**G**), selective angiography of the left SPA (**H**) and left external carotid angiography (**I**) after coil embolization of the SP and basilar plexus confirmed complete disappearance of the shunt blood flow.

Patient Informed Consent

The necessary patient informed consent was obtained in this study.

Discussion

Observations

In the AC-AVF of the present case, the peripheral branches of the bilateral internal maxillary arteries were the main feeding arteries. Typical feeding arteries of the AC-AVF are the ascending pharyngeal artery (92% of AC-AVFs), occipital artery (56.3%), meningeal branches of the vertebral artery (47.3%), and clival branches of the

meningohypophyseal trunk (21.4%). These feeding arteries, which run near the hypoglossal canal, often form bilateral feeding arteries.^{2,5} Rarely, the posterior auricular artery (13.4%), middle meningeal artery (14.3%), and internal maxillary artery (5.4%) are the feeding arteries of an AC-AVF.² Mizutani et al.¹ identified the ipsilateral sphenopalatine artery as the feeding artery in two (28.6%) of seven cases of AC-AVF on cone-beam computed tomography, and detailed analysis can relatively often identify the peripheral branches of the internal maxillary artery as the feeding artery. The peripheral part of the internal maxillary artery is called the pterygopalatine segment and runs

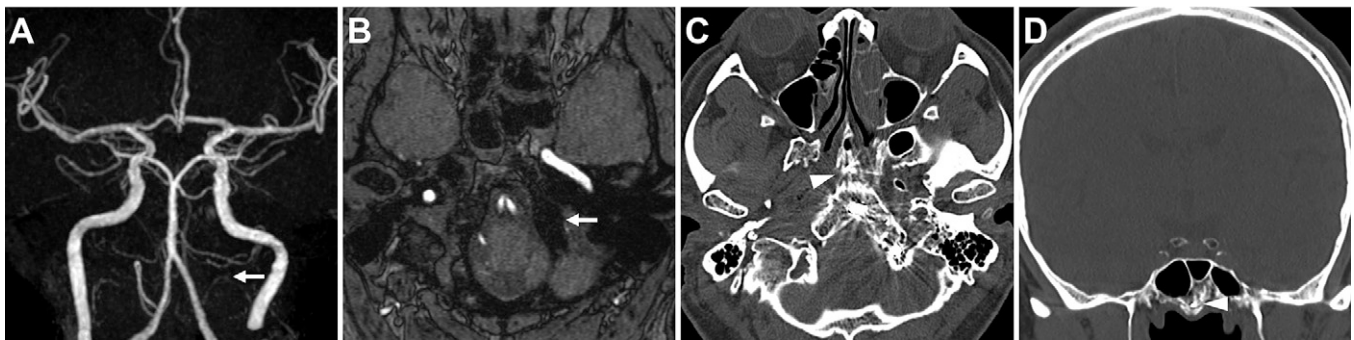


FIG. 4. Postoperative imaging findings. Magnetic resonance angiography (A) and TOF imaging (B) confirmed the disappearance of high signal intensity in the SP (arrow). Axial (C) and coronal (D) sections of CT showing coils in the feeding arteries (arrowhead) with the peripheral branches of the bilateral internal maxillary arteries gathering in the caudal sphenoid bone and also in the SP of the jugular tubercle and the clivus.

through the pterygopalatine fossa to the nasal cavity as a terminal branch of the sphenopalatine artery. In the present case, cone-beam computed tomography confirmed that the sphenopalatine artery running from the pterygopalatine segment of the internal maxillary artery through the sphenopalatine foramen, the artery of the pterygoid canal running through the pterygoid canal, and the artery of the foramen rotundum running through the foramen rotundum formed bilateral feeding arteries. Normally, the sphenopalatine artery does not flow into the cranium because it reaches the nasal cavity, but in the present case it penetrated the sphenoid bone and formed a feeding artery. The feeding arteries from the peripheral part of the bilateral internal maxillary arteries anastomosed with the cavernous sinus branch of the left middle meningeal artery and the bilateral accessory meningeal arteries in the sphenoid bone. These feeding arteries gathered in the sphenoid bone and then anastomosed with the right ascending pharyngeal artery in the clivus of the occipital bone, with the feeding arteries running a relatively long distance and flowing into the shunted pouch in the left jugular tubercle. Kulanthaivelu et al.⁶ examined the angiography images of seven cases of anterior cranial fossa AVF and confirmed that the sphenopalatine artery was the feeding artery in three (42.9%) of seven cases, suggesting that the sphenopalatine artery is the main feeding artery of the anterior cranial fossa AVF near the nasal cavity.⁷ Furthermore, in AVFs formed within the sphenoid bone, the peripheral part of the internal maxillary artery has been identified as the main feeding artery.^{8,9}

It is recognized that AVFs are triggered by trauma, infection, inflammation, surgery, tumors, venous sinus thrombosis, venous hypertension associated with venous occlusion or stenosis, and factors inducing angiogenesis.¹⁰ Considering the relatively large shunted pouch formed in the jugular tubercle and the clivus of the occipital bone and the 5-year history of tinnitus, the duration of the disease since the onset of the AC-AVF seems relatively long. Angiogenesis induced by the long-term increase in venous pressure associated with AVF may have enlarged the shunted pouch and anastomosed the peripheral part of the internal maxillary artery further away from the shunted pouch as a feeding artery. The gathering site of the feeding arteries in the present case was continuous within the occipital and sphenoid bones. Mizutani et al.¹ speculated that there are abundant intraosseous venous channels, such as the jugular tubercle venous complex, around the hypoglossal canal, and that AC-AVF is formed due to blood flow congestion and thrombosis in these intraosseous venous channels. There are also abundant venous tracts

within the clivus.¹¹ Therefore, it is possible that the venous tract congestion and thrombosis within the jugular tubercle and clivus caused a physiological anastomosis between these venous tracts and the intrasphenoidal venous tract, and that further angiogenesis led to the formation of an AVF.^{12,13} Furthermore, the patient had a history of sinusitis since adolescence, and preoperative computed tomography showed left maxillary sinusitis just anterior to the sphenopalatine foramen. It is speculated that sinusitis or infection of the skull base triggered thrombosis of the intraosseous veins, resulting in acquired AVF formation in the bone.⁸ In the present case, sinusitis may have been related to the fact that a branch vessel in the peripheral part of the internal maxillary artery, far from the jugular tubercle, became the feeding artery.

In AC-AVF, various feeding arteries and outflow veins form a rich network, and the vascular structure is complex and overlapping, making it difficult to ascertain the vascular architecture around the shunt by ipsilateral carotid angiography.² Selective microcatheterization or contralateral carotid angiography to minimize the delineation of the arteries around the shunt as much as possible can be useful to obtain an accurate delineation of the fistulous point.^{14–16} In the present case, it was difficult to delineate the fistulous point and the shunted pouch in detail by ipsilateral external carotid angiography (Fig. 2A), but the gathering site of the feeding arteries and the shunted pouch were clearly delineated by contralateral external carotid angiography and selective angiography of the sphenopalatine artery (Fig. 2E and G). In the present case, the feeding arteries of the contralateral external carotid artery gathered in one site, so there was no significant difference in the depiction of the gathering site and the shunted pouch when comparing external carotid angiography and selective angiography of the sphenopalatine artery, but the usefulness of selective angiography is suggested in cases with diffuse inflow into the shunted pouch. Furthermore, because the sphenopalatine artery is a terminal branch of the internal maxillary artery, there is no need to select the branch to guide microcatheters into the internal maxillary artery. In the present case, insertion of the microcatheter at the deepest part of the gathering site of the feeding arteries was identified on selective angiography of the contralateral sphenopalatine artery, allowing dense embolization of the gathering site of the feeding arteries and elimination of shunt blood flow from it (Fig. 3C–E).

In general, AC-AVF has a rich network in the outflow veins, resulting in various access routes to the shunted pouch.² In the present

case, there was outflow from the shunted pouch, primarily to the basilar plexus and anterior condylar vein, and access to the shunted pouch via the basilar plexus was considered the first choice for causing the ocular symptoms. Access from the femoral vein to the right inferior petrosal sinus or right external jugular vein to the basilar plexus and the shunted pouch was difficult. Furthermore, access to the anterior condylar vein and the shunted pouch via the vertebral venous plexus or deep cervical vein was also difficult. Finally, the shunted pouch could be reached via the facial vein, superior ophthalmic vein, cavernous sinus, and basilar plexus by inserting a sheath directly into the right external jugular vein. A case of an AC-AVF has been reported, in which the superior ophthalmic vein was surgically exposed at the supraorbital margin followed by direct puncture of the superior ophthalmic vein to reach the shunted pouch and densely embolize the shunt.¹⁷ However, in addition to cosmetic problems, this method of direct puncture of the superior ophthalmic vein exposed by resection may cause bleeding and difficulty in identification of the superior ophthalmic vein, supraorbital nerve injury, and eyelid elevator muscle injury.¹⁸ To our knowledge, no case has been reported in which direct puncture of the external jugular vein was used to access the shunted pouch of an AC-AVF and embolization was safely achieved. When a sheath is inserted directly into the external jugular vein, the interference between the distal access catheter and the guide catheter caused by the difference in catheter length is eliminated, allowing the small-diameter distal access catheter to reach as far as possible. With adequate support from the distal access catheter, the microcatheter easily reached the shunted pouch, turned in the shunted pouch, and was guided deep into the gathering site of the feeding arteries, resulting in dense embolization of the gathering site.

Lessons

Selective angiography of the contralateral sphenopalatine artery may be useful to confirm the gathering site of the peripheral branches of the bilateral internal maxillary arteries in an AC-AVF.

Acknowledgments

The authors would like to thank Ms. Miho Kobayashi for the English language editing.

References

- Mizutani K, Akiyama T, Minami Y, et al. Intraosseous venous structures adjacent to the jugular tubercle associated with an anterior condylar dural arteriovenous fistula. *Neuroradiology*. 2018;60(5):487–496.
- Spittau B, Millán DS, El-Sherifi S, et al. Dural arteriovenous fistulas of the hypoglossal canal: systematic review on imaging anatomy, clinical findings, and endovascular management. *J Neurosurg*. 2015;122(4):883–903.
- Crockett MT, Chiu AHY, Singh TP, McAuliffe W, Phillips TJ. Transvenous coil embolization with intra-operative cone beam CT assistance in the treatment of hypoglossal canal dural arteriovenous fistulae. *J Neurointerv Surg*. 2019;11(2):179–183.
- Hellstern V, Aguilar-Pérez M, Schob S, et al. Endovascular treatment of dural arteriovenous fistulas of the anterior or posterior condylar vein: A cadaveric and clinical study and literature review. *Clin Neuroradiol*. 2019;29(2):341–349.
- McDougall CG, Halbach VV, Dowd CF, Higashida RT, Larsen DW, Hieshima GB. Dural arteriovenous fistulas of the marginal sinus. *AJNR Am J Neuroradiol*. 1997;18(8):1565–1572.

- Kulanthavelu K, Pendharkar H, Prasad C, et al. Anterior cranial fossa dural arteriovenous fistulae—angioarchitecture and intervention. *Clin Neuroradiol*. 2021;31(3):661–669.
- Salvati LF, Palmieri G, Minardi M, Bianconi A, Melceme A, Garbossa D. Foramen caecum vein involved in dural arteriovenous fistula fed by sphenopalatine arteries: a case report. *NMC Case Rep J*. 2021;8(1):371–376.
- Mohimen A, Kumar Kannath S, Jayadevan ER. Skull base osseous arteriovenous fistula—a rare clinical entity: Case report and literature review. *World Neurosurg*. 2017;97:760.e9–760.e12.
- Park ES, Jung YJ, Yun JH, Ahn JS, Lee DH. Intraosseous arteriovenous malformation of the sphenoid bone presenting with orbital symptoms mimicking cavernous sinus dural arteriovenous fistula: a case report. *J Cerebrovasc Endovasc Neurosurg*. 2013;15(3):251–254.
- Reynolds MR, Lanzino G, Zipfel GJ. Intracranial dural arteriovenous fistulae. *Stroke*. 2017;48(5):1424–1431.
- Mizutani K, Toda M, Kurasawa J, et al. Analysis of the venous channel within the clivus using multidetector computed tomography digital subtraction venography. *Neuroradiology*. 2017;59(3):213–219.
- Terada T, Higashida RT, Halbach VV, et al. Development of acquired arteriovenous fistulas in rats due to venous hypertension. *J Neurosurg*. 1994;80(5):884–889.
- Kutluk K, Schumacher M, Mironov A. The role of sinus thrombosis in occipital dural arteriovenous malformations—development and spontaneous closure. *Neurochirurgia (Stuttg)*. 1991;34(5):144–147.
- Kiyosue H, Tanoue S, Okahara M, Mori M, Mori H. Ocular symptoms associated with a dural arteriovenous fistula involving the hypoglossal canal: selective transvenous coil embolization. Case report. *J Neurosurg*. 2001;94(4):630–632.
- Choi JW, Kim BM, Kim DJ, et al. Hypoglossal canal dural arteriovenous fistula: incidence and the relationship between symptoms and drainage pattern. *J Neurosurg*. 2013;119(4):955–960.
- Miyachi S, Ohshima T, Izumi T, Kojima T, Yoshida J. Dural arteriovenous fistula at the anterior condylar confluence. *Interv Neuroradiol*. 2008;14(3):303–311.
- Tanoue S, Goto K, Oota S. Endovascular treatment for dural arteriovenous fistula of the anterior condylar vein with unusual venous drainage: report of two cases. *AJNR Am J Neuroradiol*. 2005;26(8):1955–1959.
- Biondi A, Milea D, Cognard C, Ricciardi GK, Bonneville F, van Effenterre R. Cavernous sinus dural fistulae treated by transvenous approach through the facial vein: report of seven cases and review of the literature. *AJNR Am J Neuroradiol*. 2003;24(6):1240–1246.

Disclosures

The authors report no conflict of interest concerning the materials or methods used in this study or the findings specified in this paper.

Author Contributions

Conception and design: Ikeda, Kinosada. Acquisition of data: Ikeda, Hata. Analysis and interpretation of data: Ikeda. Drafting the article: Ikeda, Kimura, Kurosaki. Critically revising the article: Ikeda, Kimura, Nishi, Uezato. Reviewed submitted version of manuscript: Ikeda, Kinosada. Approved the final version of the manuscript on behalf of all authors: Ikeda. Administrative/technical/material support: Ikeda. Study supervision: Chin.

Correspondence

Hiroyuki Ikeda: Kurashiki Central Hospital, Kurashiki, Okayama, Japan. hiroyuki.ikeda930@gmail.com.